Microplastics: diffusion into ocean floors and methodology for age determination

*Kiichiro Kawamura[1]

1. Yamaguchi University

Plastic pollution in oceans is a significant social problem. It is current symbolic scenery that many plastic bottles are washed ashore at the Sea of Japan.
These plastic materials are ordinarily crashed to be microplastics that are disseminated into all the oceans. These microplastics adhered pollutants (e.g. PCB) are accumulated in marine creatures. Such plastic pollutions in oceans are investigated in shallow water depths, but it is unclear in deep-seas deeper than several thousands meters.
On the other hand, microplastics can use as an index fossil. Radionuclide is one of the famous examples for age determination using artifacts. For example, we use 134Cs and 137Cs for age determination. 134Cs of about 2 years in a half life can be used an index of nuclear tests and nuclear power plant accidents. It plays an important role in the Fukushima Daiichi nuclear power plant accident (e.g. Oguri et al., 2013; Sci. Rep.). 137Cs of about 30 years in a half life can detect the accident ages from sediments for relatively long time. The famous peaks of 137Cs are nuclear tests in 1960s, the Chernobyl disaster in 1987 in sediments.
Microplastics are a similar artifact. According to the Vinyl Environmental Council, plastic products have increased rapidly from 100 million tons / yr in 1960s to 200 million tons / yr in 1991. But recently these have been 180 million tons / yr since 2008. These products and their particles as microplastics would accumulate continuously without any decaying, but it is unclear.
The aim to this study is 1) to know a spatial distribution of microplastics in surface sediments collected from deep-sea floor as several thousands meters in water depth, and 2) to know a vertical distribution of them. The first aim is to know a marine pollution degree of microplastics, and the second aim is to establish age determination using microplastics.

Keywords: Sediment age, microplastic, Surface sediments

The significant of the sedimentary system in the southwest Ryukyu Trench in terms of Source-to-Sink

*KanHsi Hsiung[1], Toshiya Kanamatsu[1], Ken Ikehara[2], Kazuya Shiraishi[1], Kazuko Usami[2]

1. Japan Agency for Marine-Earth Science and Technology, 2. National Institute of Advanced Industrial Science and Technology

The southwest Ryukyu Trench near Taiwan is an ideal place for source-to-sink studies because the linkage between the terrestrial sediment source of Taiwan and the marine sink in Ryukyu Trench within a short distance can be determined. This study aims to improve our understanding of the oceanic trench sedimentary system. Using bathymetry, seismic reflection data and cored samples in the southwest Ryukyu Trench areas, we determine distinct features of the submarine canyons, trench wedge, bathymetric ridges and fore-arc basins which are linked together to form two sediment dispersal systems. Two sediment dispersal systems can be identified. First, the trench end sediment dispersal system is characterized by the longitudinal sediment dispersal to the southwestern end of Ryukyu Trench via the Hualien Canyon with additional lateral sediment supplies from the Taitung Canyon merging into the lower Hualien Canyon. This system allows Taiwan orogenic sediments transported far-field and to feed sediments longitudinally to the southwest Ryukyu Trench end. This type of longitudinal sediment dispersal demonstrates a link of sediment of land drainage (source) to the far-field deep oceanic trenches (sink) via networks of submarine canyons. Sediments derived from Taiwan orogen mainly transported downslope by submarine canyons are blocked by the Gagua Ridge. Second, the forearc sediment dispersal system consists of the transverse sediment dispersal from the Ryukyu islands down-slope to forearc basins including Hoping, Nanao, East Nanao and Hateruma. Most of the down-slope sediments from Ryukyu islands are blocked by the W-E trending Yaeyama Ridge along the trench slope break and trapped sediments in the forearc basins. The Yaeyama Ridge is considered as a sediment barrier for sediments sourced by the Ryukyu Islands to be transported to the Ryukyu Trench.

Keywords: Sediment transport, Seismic characteristics, Source-to-Sink, Southwest Ryukyu Trench, Taiwan

Interaction of forearc basin stratigraphy with growth of accretionary wedge: Insights from numerical simulations

*Atsushi Noda[1]

1. National Institute of Advanced Industrial Science and Technology

Forearc basins are important elements along subduction zones; their deposits and structures recorded various events in history at a high resolution. However, forearc basins have received relatively less attention than the deformation front, because their formations depend on complex interactions among uplift/subsidence of backstop, growth/shrink of accretionary wedge, subducting oceanic slab, and covering sediments. It is often difficult to evaluate influence of each factor. In accretion-dominated margins, forearc basins commonly develop on or beside accretionary wedges, indicating growth patterns of the wedge may be primary controllers of the basin formations. Because material fluxes between the boundary of overriding and subducting plates highly influence the wedge growth patterns, They must be also important for development of forearc basins. The aim of this study is to understand formation of forearc basin stratigraphy in terms of sediment fluxes in subduction zones. I performed numerical simulations to reproduce forearc basins formed between growing accretionary wedges and continental backstops. The simulations assumed that sediments filling forearc basin (Q_{inFAB}) were determined by balance among sediment supply to the basin (Q_s), trench fill sediments (Q_{inT}), and subducting sediments from the trench into subduction channel (Q_{outT}). The sediment fluxes of Q_s, Q_{inT}, and Q_{outT} were independently fluctuated, and sediments accreted to the wedge (Q_{inAC}) was Q_s - Q_{inFAB} + Q_{inT} - Q_{outT}. Two models of constant and dynamic taper angles of the wedges were tested. In the dynamic taper model, the taper angle (θ) relied on pore pressure ratios of the wedge interior and the basal detachment, which were functions of Q_{inAC} and Q_{outT}, respectively.

The constant taper models showed positive relationships between Q_{inFAB} with Q_{total} (= Q_s + Q_{inT} −Q_{outT}) or Q_{inAC}. Underfilled basin could exist only when Q_s was smaller than depositional area produced by the wedge growth. At a time of transition from underfill to overfill, trajectories of Q_{inFAB} and Q_{inAC} broke and then returned to the equilibriums with some fluctuations. The dynamic taper models also showed linear relationships between Q_{inFAB} and Q_{total}, although Q_{inAC} and Q_{inFAB} relationships were much more scattered than the constant taper models. A prominent feature of the dynamic taper model was a negative relationship between time-averaged differences of Q_{inAC} and Q_{inFAB}, when θ was increasing or decreasing. The sediment input rates to the basins (Q_{inFAB}) decreased, even though those to the wedge (Q_{inAC}) increased with reducing θ. Similar negative relationships could be observed during increase of θ. These results suggest that growing wedge with changing the taper angle significantly affects the basin stratigraphy. Two end members of the wedge-growth patterns can be considered; (1) progradation by frontal accretion with decreasing θ and (2) vertical growth by basal accretion or thickening by splay faults with increasing θ. For the former type (1), most of Q_{inT} are consumed for progradation of the wedge to approach the reduced θ, resulting in slower sedimentation rate and then occurrence of a condensed section or an unconformity, even though sufficient Q_s is supplied to the basin. The latter type (2) yields more space for sedimentation landward side of the wedge due to uplift of the outer arc high, which leads to faster sedimentation rate or occurrence of an underfilled basin, depending on Q_s.

Keywords: forearc basin, accretionary wedge, sediment flux, subduction zone

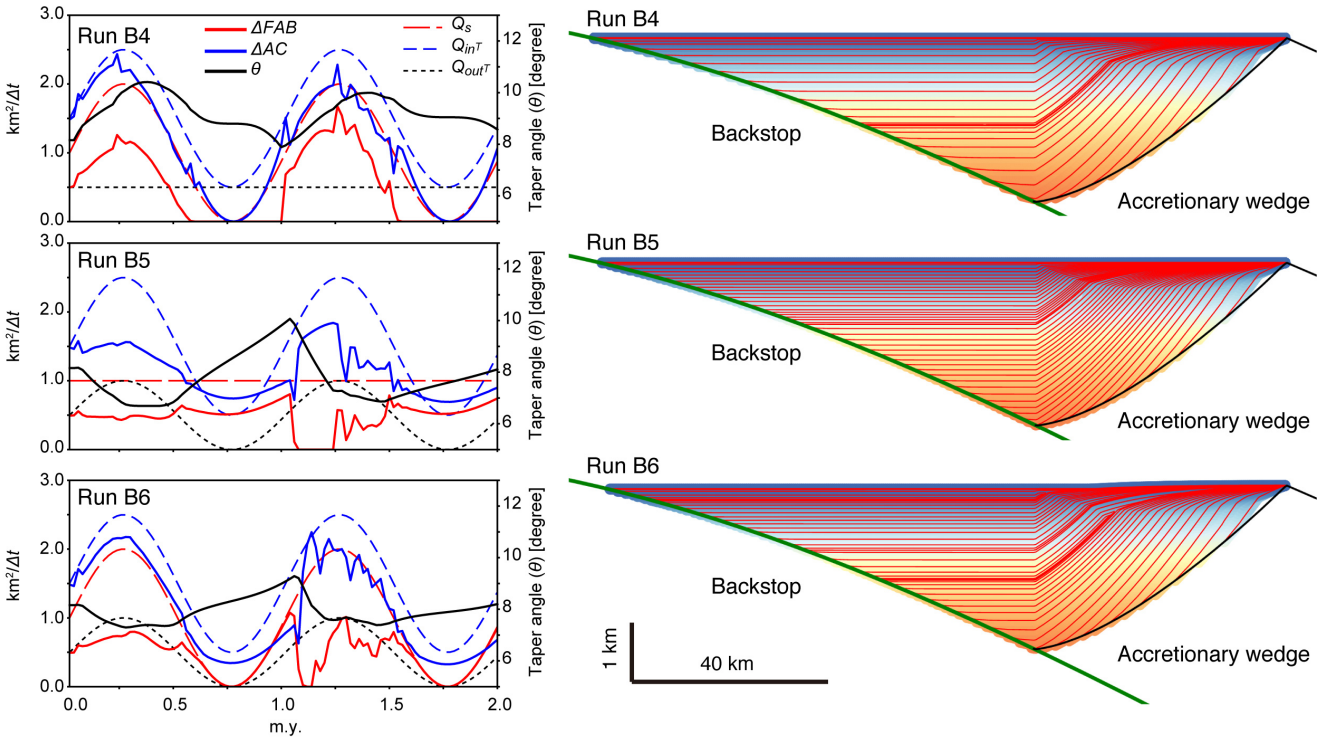

Fig. 1: Selective examples from the dynamic taper models. (Left) Diagrams for initial parameters of Q_s, Q_{in_T}, and Q_{out_T} (see the text for notations), taper angles (θ), and increased areas of forearc basin (ΔFAB) and accretionary wedge (ΔAC) at each time step. (Right) Resultant stratigraphy of forearc basins.

Inverse analysis of tsunami deposits using non-steady flow model

*Hajime Naruse[1], Tomoya Abe[2]

1. Department of Geology and Mineralogy, Graduate School of Science, Kyoto University, 2. Geological Survey of Japan, AIST

Tsunami deposits provide important clues to understand ancient tsunami events. Here we propose a new inverse model of tsunami deposit emplacement. The model is an improved version of FITTNUSS that is the inversion model proposed by the authors. The model considers both transport of non-uniform suspended load and entrainment of basal sediments, and the flow deceleration process is newly incorporated in this model. This inversion model requires the spatial distribution of deposit thickness and the pattern of grain-size distribution of the tsunami deposit along 1D shoreline-normal transect as input data. It produces as output run-up flow velocity, inundation depth and concentration of suspended sediment. To solve for advection of non-uniform suspended load, a transformed coordinate system is adopted, which increase computational efficiency. Tests of inversion using artificial data successfully allow reconstruction of the original input values, suggesting the effectiveness of our optimization method. We apply our new inversion model to the 2011 Tohoku-Oki Tsunami deposit on Sendai Plain, Japan. The thickness and grain-size distribution of the tsunami deposit was measured along a 4 km long transect normal to the coastline. The result of our inversion fits well with the observations from aerial videos and field surveys. We conclude that this method is suitable for the analysis of ancient tsunami deposits, and that it has the advantage of requiring the minimum information about the condition of the emplacing paleotsunami for reconstruction.

Keywords: tsunami, tsunami deposit, inverse analysis

Reconstruction of flow depth and velocity of tsunamis by inverse analysis using thickness and grain-size distribution of tsunami deposits along 1D transect: Application to the 2011 Tohoku-oki tsunami and the 869 Jogan tsunami

*Tomoya Abe[1], Hajime Naruse[2], Daisuke Sugawara[3]

1. Geological Survey of Japan, AIST, 2. Department of Geology and Mineralogy, Graduate school of Science, Kyoto University, 3. Museum of Natural and Environmental History, Shizuoka

A new inversion model FITTNUSS (Framework of Inversion of Tsunami deposits considering Transport of Non-uniform Unsteady Suspension and Sediment entrainment) was proposed for estimation of tsunami hydrodynamic conditions from characteristic features of tsunami deposits along the transect. The forward model designed for the inverse analysis considers transport of non-uniform suspended load, and deposition from both run-up and stagnant phases of the tsunamis are calculated. The inversion model requires thickness and grain-size distribution of the tsunami deposit along 1D shore-normal transect as input data, and calculates flow depth, flow velocity and concentration of suspended sediments. Here, we applied this inversion model to the modern and the ancient tsunami deposits emplaced in the same region, and compare the reconstructed flow properties for understanding the behavior of the past tsunami. Firstly, the inversion model was applied to the 2011 Tohoku-oki tsunami deposit in the northern part of Sendai Plain. Thickness and grain-size distribution of the tsunami deposit were measured along the 4 km long transect from shoreline to the inundation limit. The run-up flow velocity observed by video footage was 4.2 m/s on average (Hayashi and Koshimura 2013), while the value estimated by the model was 4.15 m/s. The flow depths near shoreline obtained by the field survey and the inverse analysis were 4.9 m and 4.71 m, respectively. Secondly, the inversion model was applied to the 869 Jogan tsunami deposit in the northern part of Sendai Plain. Thickness and grain-size of the tsunami deposit were observed along the 3 km long transect from the paleo-shoreline to the estimated inundation limit. The run-up flow velocity and flow depth were estimated as 6.3-8.8 m/s in average and 5.3-7.8 m near shoreline. Although the 2011 Tohoku-Oki earthquake is often considered as the recurrence of the 869 Jogan Earthquake, the reconstructed values of flow velocity and depth of the 869 Jogan tsunami in the northern part of Sendai Plain were significantly high and deep in comparison with those of the 2011 Tohoku-oki tsunami, suggesting that there could be considerable differences in their generating mechanisms or topographic settings between these two tsunami events.

Keywords: tsunami deposit , flow depth, flow velocity, inverse analysis, 2011 Tohoku-oki tsunami, 869 Jogan tsunami

Controls of Ice Cover on Arctic Delta Morphodynamics and Depositional Processes

*YeJin Lim[1], Joseph Levy[2], Timothy Goudge[1], Wonsuck Kim[1]

1. University of Texas at Austin, 2. University of Texas Institute for Geophysics

Deltas are dynamic systems that can provide important information on past environmental conditions. Arctic deltas in particular have the potential to preserve critical information about climate change in one of the most temperature-sensitive regions of the Earth. Despite the fact that the responses to climate change in the Arctic can significantly affect deltaic morphology, Arctic deltas have largely been neglected as records of climate conditions, and the mechanism(s) by which ice cover alone produces the resultant delta morphology unique to Arctic deltas remains unexplained. We have performed laboratory experiments to directly evaluate the key controls of ice cover on delta morphodynamics and associated depositional processes to identify signatures of ice cover presence during deposition. Our results show that ice cover drives spatially varying sediment transport on the subaqueous delta clinoform through sub-ice channels, which leads to the development of (1) extended delta lobes built by elongated, subaqueous sediment wedges and (2) highly variable bathymetry with increasing topographic roughness up to a water depth above which bottom-fast ice cover exists. The results of our laboratory experiments provide evidence for the effects of ice cover on delta sediment transport and depositional processes, and predictions for changes to delta morphology in the presence of ice cover during deposition. Notably, the unique seascape features of ice-covered deltas may serve as diagnostic geomorphic markers of cold climate conditions where ice cover exists, and hence, as indicators of climate change captured on Arctic coasts. Therefore, Arctic deltas can potentially be a valuable tool for developing geomorphic models to understand and predict coastal landscape changes in the sensitive Arctic where more rapid and much larger changes (e.g., ice cover, temperature, and sea level) are projected in response to climate change.

Keywords: Arctic deltas, Deltas, Arctic, Climate change, Experimental study

Effect of basin water depth on the morphodynamics of delta distributary channels: A tank experiment

*Tetsuji Muto[1]

1. Department of Environmental Science, Nagasaki University

Recent experimental studies of river deltas have brought a new view that the morphodynamics of distributary channels is seriously affected by basin water depth. In a delta fronting on an extremely deep water, so that the delta cannot prograde, its distributary channels tend to be stabilized in the form of an axial valley and become graded. On the other hand, if the basin water is extremely shallow, the delta’s distributary channels keep autocyclic shifting and are never stabilized. These two extreme examples imply that there exist a spectrum of "intermediates" showing different channel behaviors in response to different basin water depths. The present study challenges to find some characteristic forms of "intermediates" and grasp the whole picture of the spectrum, based on the analytical results of a series of experimental runs that were conducted with different basin water depths of 1 cm, 1.5 cm, 2.67 cm, 4.0 cm and 20 cm, but with the same basement configuration, the same water discharge and the same sediment supply rate. The results of the runs suggest that with moderately deep basin water in front, there can develop a single, quasi-stabilized major channel accompanied by multiple minor channels which are also quasi-stabilized.

Keywords: alluvial grade, autocyclic, basin water depth, channel stability, delta , experiment

Analytical and experimental study of dual-slope effects on Gilbert and hyperpycnal deltas over bedrock

*Steven Y. J. Lai[1], Yung-Tai Hsiao[1], Chia-Chi Chang[1], Yi-Juei Chiu[1], Fu-Chun Wu[2]

1. National Cheng Kung University, 2. National Taiwan University

Deltas preserve a vast of sediment prism at the shoreline at different spatiotemporal scales and with diverse environmental settings. The sediment prism subjects to homopycnal (or hypopycnal) flows usually yields a Gilbert-type delta, which has an upward-concaved mild topset, a steep foreset rested at the angle of repose and a relatively flat bottomset. Unlike Gilbert deltas, the sediment prism formed by hyperpycnal flows (or turbidity currents) may yield a delta with its subaqueous foreset upward-concaved and bed slope much milder than the angle of repose. However, our knowledge about the morphodynamics of deltas that prograde over bedrock basements with different subaerial and subaqueous slopes is still lacking. In this study, we investigate the effects of the subaerial and subaqueous basement slopes on Gilbert and hyperpycnal deltas by using analytical and experimental approaches. We propose two newly derived analytical solutions for describing the formation of Gilbert and hyperpycnal deltas over different dual-slope settings, respectively. The exact solutions are quantitatively verified by well-controlled physical experiments, and yield good agreements in both delta profiles and moving trajectories: bedrock-alluvial transition and shoreline. Under constant influx conditions, the scaled delta profiles at different times collapse to a single profile, confirming that the morphological self-similarity would establish over single-slope or dual-slope basements, thus enabling us to use the analytical similarity solutions as a tool for quantifying the relative effects of dual-slope to single-slope basement. Our results reveals that the effects of the subaerial and subaqueous slopes are asymmetric for both Gilbert and hyperpycnal deltas. An increase of the subaerial slope would push the delta forward and upward, leading to an enhanced forward migration of shoreline, a raised yet compressed topset, and a suppressed headward migration of bedrock-alluvial transition. On the contrary, an increase of the subaqueous slope would pull down the delta, suppressing the headward migration of bedrock-alluvial transition, forward migration of shoreline and topset dimensions while increasing the foreset length. Thus, with our analytical framework and in light of the scale independence of delta morphology, our results are likely to apply beyond experimental scales.

Keywords: Gilbert delta, hyperpycnal delta, dual-slope, self-similarity, analytical solution, physical experiment

Bankfull characteristics of alluvial rivers: evolution toward macroscopic equilibrium

*Kensuke Naito[1], Gary Parker[1,2]

1. Department of Civil and Environmental Engineering, University of Illinois at Urbana-Champaign, 2. Department of Geology, University of Illinois at Urbana-Champaign

Alluvial rivers are often characterized in terms of their bankfull characteristics (i.e. bankfull discharge, bankfull width, bankfull depth, and channel slope). Studies on bankfull hydraulic geometry relations have shown that bankfull characteristics change in a consistent way with bankfull discharge. This suggests that if bankfull discharge is changed, bankfull geometry should change accordingly. Another problem of interest is the recurrence interval of bankfull discharge, which is often found to be 1 to 2 years. None of these studies, however, reveals what determines bankfull discharge to begin with. As a result, the parameters which determine bankfull characteristics and processes remain unknown. A better understanding of bankfull characteristics would lead to better prediction of how bankfull characteristics change. This knowledge is of great usefulness in many fields including geomorphology, engineering, ecology, and water management. In this study, we propose a framework for the establishment of and evolution to bankfull characteristics of alluvial rivers. It is commonly accepted that an alluvial river should self-evolve toward an equilibrium state, in which the net sediment flux within the reach of interest is zero. Applying this concept, we anticipate that such an equilibrium channel is able to maintain the balance between the fine sediment that is deposited onto the floodplain due to overbank flow (referred as floodplain construction herein) and the fine sediment that is removed from the floodplain throughout lateral channel migration (referred as floodplain destruction herein). Lateral channel migration leads to floodplain destruction because of the average elevation difference prevailing between the (older, thus thicker) outer eroding bank and the (freshly-deposited, thus thinner) inner depositing bank. The equilibrium channel must also be able to transport the supply of bed material without causing overall aggradation or degradation of the reach. In order to quantify floodplain construction and destruction, as well as the bed material sediment transport rate, we use a flow duration. We use this proposed framework to develop a numerical model to find the reach-average equilibrium bankfull characteristics for specified flow duration curve and bed material supply rate. The model not only predicts equilibrium, but can also be used to investigate the adjustment time scale of the system from one equilibrium state to another when it is disturbed. In the model, bankfull width adjustment is accomplished by modeling outer bank erosion and inner bank deposition independently; if outer bank erosion occurs at a faster rate than inner bank deposition, bankfull width increases in time. Bankfull depth adjustment is accomplished by modeling the morphodynamics of fine sediment, which deposits onto the floodplain, and the morphodynamics of bed material. That is, if the incoming bed material discharge is greater than outgoing bed material discharge, the channel bed of the reach in question should increase in elevation, leading to a decrease in bankfull depth. Likewise, if the effect of floodplain construction is greater than that of floodplain destruction, bankfull depth would increase. At the equilibrium state, the reach-averaged rate of outer bank erosion and inner bank deposition are expected to be the same, and the inflowing transport rates of both bed material and fine sediment should be equal to their corresponding outflowing values over a reach of interest. The model is applied to the Minnesota River near Jordan, MN, USA, in order to demonstrate the response of the system to changes in e.g. sediment supply rate and flow duration curve.

Keywords: Bankfull characteristic, Alluvial river, Overbank floodplain deposition, Lateral channel migration

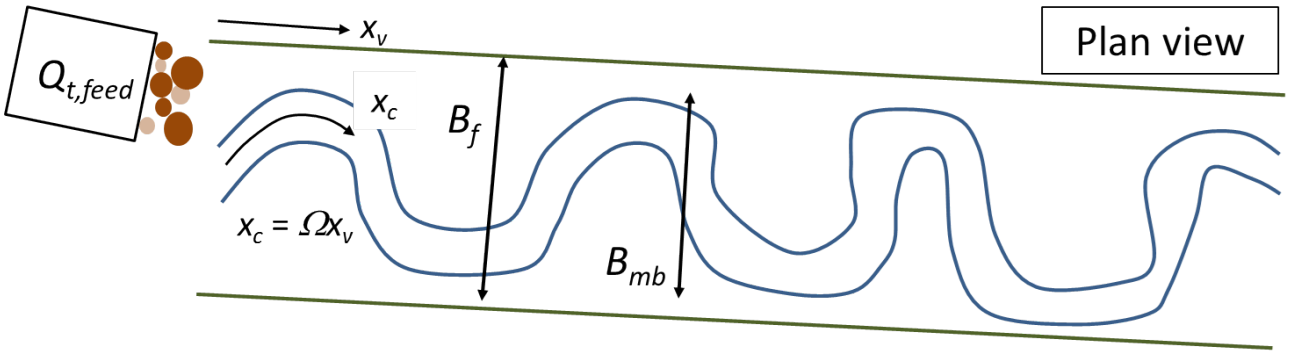

Cross section

$$H_{bf} = H_c + H_n$$

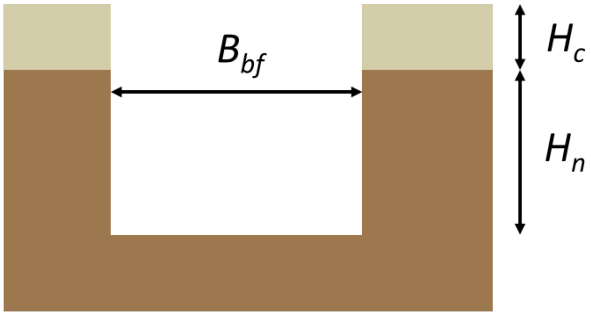

B_{bf}: Bankfull width [L]
B_f: Floodplain width [L]
B_{mb}: Meander belt width [L]
H_{bf}: Bankfull depth [L]
H_c: Upper cohesive layer thickness [L]
H_n: Lower non-cofesive layer thickness [L]
$Q_{t,feed}$: Bed material supply [L^3/T]
Ω: Channel sinuosity [1]

Evaluation of Properties of Bed Phase Transition by the Discriminant Analysis of Experimental and Field Data Sets

*Koji Ohata[1], Hajime Naruse[1], Miwa Yokokawa[2]

1. Kyoto University, 2. Osaka Institute of Technology

This study provides the quantitative evaluation for modes of the bed-phase transition of bedforms formed by unidirectional flows. Understanding the formative conditions of fluvial bedforms is significant for geological studies, and diagrams showing formative conditions of bedforms have been widely used for analyses of sedimentary structures. However, threshold conditions of bedform formation were not examined quantitatively in previous studies.

In this study, we propose discriminant functions of bedform existence fields in dimensionless parametric space by means of the discriminant analysis using the Mahalanobis distance. We analyzed 3401 existing laboratory and field observation data, and produced new bedform stability diagrams. The discriminant functions of bedform existence fields proposed in this study can be used to evaluate the properties of boundaries between bedform stability fields in terms of error rates of the analysis. Two kinds of the error rates of the discriminant analysis are obtained from (1) ratio of misclassified data and (2) results of cross-validation (the leave-one-out method). For example, as a result of the discriminant analysis, it was indicated that the apparent error rates differ depending on the bedform regimes. The apparent error rates are low at the boundaries between the the lower regime and the transition regime, whereas they are high at the boundaries between the transition regime and the upper regime. The theoretical analysis of Izumi and Parker (2009), which used the weakly non-linear stability analysis of bedforms, might explain the reason why the boundaries between the transition regime and the upper regime are not defined clearly. They predicted that there are hysteresis in the threshold conditions between plane beds and antidunes, and this hysteresis can derive the overlapped region in the laboratory observation data. In this way, our method derives the threshold conditions without any assumptions, providing means for verifying the theoretical examinations.

Reference

Izumi, N., and G. Parker (2009), The bifurcation pattern of the flat bed and antidune transition [in Japanese with English abstract], in *Proceedings of Hydraulic Engineering*, vol. 53, pp. 733–738, Japan Society of Civil Engineers.

Keywords: bedforms, discriminant analysis

The role of grain to grain interactions and turbulence in sediment transport

*Elowyn Yager[1], Mark Schmeeckle[2]

1. University of Idaho, Civil Engineering, Center for Ecohydraulics Research, 2. Arizona State University, School of Geographical Sciences and Urban Planning

Bedload transport impacts sedimentary records as well as channel and delta morphology. Predictions of the onset of sediment motion are notoriously difficult and recent studies have focused on the detailed mechanics of grain movement to improve larger scale sediment flux estimates. In particular, the importance of the duration and magnitude of flow turbulence events that drive grain motion, or the intergranular dynamics that resist sediment movement have been highlighted as being fundamentally important. Despite such recent advances, few studies directly investigate the coupling of these driving and resisting mechanics. Here we use a combination of Discrete Element Method (DEM) modeling and laboratory flume experiments to elucidate the feedbacks between grain to grain interactions and flow turbulence. In the laboratory, we conducted a set of runs in which we measured gravel transport rates for a range of applied shear stresses using a high-speed video (250 frame/s) taken from above the flume. Spectral analysis of the bedload transport time series revealed that sediment movement did not follow the well-known turbulence energy cascade and in some cases scaling between power spectral density and frequency was absent. Such a lack of scaling at some frequencies implies that grain to grain interactions are obscuring the signal of turbulence in bedload transport rates, and flow turbulence alone will not adequately describe sediment transport. To further investigate this we conducted a set of DEM model runs in which we placed a test sphere on a bed of other spheres and applied forces to the test sphere to cause its motion. The model tracked sphere positions and velocities, as well as the force chains between any interacting spheres. Between different model runs, we applied three different random sequences of fluctuating forces on the test sphere. The test sphere was immobile for one of the runs despite all applied force distributions having the same mean force and maximum impulse. In this one run, movement did not occur because the sequence of applied forces caused the test sphere to move in a way that altered the intergranular arrangement of the bed. For example, particle rearrangement in this run caused a lower bed porosity that effectively increased the forces resisting test sphere motion that could not be overcome by subsequent applied forces. If we had separately considered the effects of intergranular dynamics or flow turbulence, we would have incorrectly predicted the mobility of the test sphere. Taken together, our laboratory and DEM model results demonstrate that sediment transport calculations must include both of these two effects and in particular, how the applied and resisting forces on grains interact to control motion.

Keywords: Sediment transport, Turbulence, Intergranular friction, Morphology

Experimental Investigation of Vertical Concentration Profile and Entrainment Rates of Mixed Grain-size Particles in Turbidity Currents

*Yao Qifeng[1], Hajime Naruse[1]

1. Graduate School of Science, Kyoto University

Turbidity currents in the ocean and lakes are driven by excess density originated from suspended sediment. The dynamics of turbidity currents are largely governed by suspended sediment that is entrained from the bed. Therefore, we conducted the flume experiments of turbidity currents in order to obtain better prediction of transport rates of suspended sediment, especially focusing on differences between single and mixed grain-size cases. The vertical profiles of velocity and sediment concentration of turbidity currents containing mixed grain-size particles are the first subject of this research, which is one of the key parameters in morphodynamic models of turbidity currents. Also, a key feature for the prediction of suspended load is the description of the entrainment rate of basal sediment into suspension at the solid-fluid interface, which is the second subject of this research. The lightweight plastic particles were used in our experiments in order to reproduce suspension in relatively small scale flume (4 m long and 15 cm wide). In this research, plastic particles with the gravity of 1.45 were chosen as the model sediment material. As the focus of the experiments reported here was centered on the dynamics of the current body, rather than the head, care was taken to measure only after the current front had passed and the flow had achieved a quasi-equilibrium state.

Firstly, we report vertical profile of concentration of mixed grain-size sediments in experimental turbidity currents. For the experiments using uniform and nonuniform sediment, the vertical profiles suggested that the distribution of concentration of finer particles is less stratified than the coarser particles, and finer particles have more capability to diffuse upward, which tends to approximately uniform distribution above a certain height. Comparing to the result of Sequeiros et al. (2010), the vertical profiles of dimensionless distribution of suspension concentration shows no significant difference between uniform and mixed-grain sediments, which represented the vertical profiles of concentration of particles have identical assessment between turbidity currents and dense saline underflows.

Secondly, we examined the entrainment rate of basal sediment to suspension in turbidity currents, and compared our measurements with the prediction using the empirical formulation proposed by Garcia and Parker (1991, 1993). In the uniform particle experiments, the prediction of entrainment of sediment is consistent with the measurement accurately, whereas in the mixed grain-size particle experiments, it represent less consistent to anticipation. This implies that the new empirical formulation is needed for predicting entrainment rate of the mixed grain-size sediments into suspended load.

References

Garcia, M., and Parker, G. (1991). ‘‘Entrainment of bed sediment into suspension.’’ *J. Hydraul. Eng.,* 117(4), 414–435.

Garcia, M., and Parker, G. (1993). ‘‘Experiments on the entrainment of sediment into suspension by a dense bottom current.’’ *J. Geophys. Res.,* 98(3), 4793–4807.

Sequeiros, O.E., et al. (2010). “Characteristics of velocity and excess density profiles of saline underflows and turbidity currents flowing over a mobile bed.” *J. Hydraul. Eng.*, 136(7), 412-433.

Keywords: flume experiment, mixed grain-size particles, vertical concentrantion profile, entrainment rate

Preservation of transient flow conditions in wave ripple defects

*Kimberly Huppert[1], J. Taylor Perron[1], Paul M. Myrow[2], Abigail R. Koss[3], Andrew D. Wickert[4]

1. Dept. of Earth, Atmospheric, and Planetary Sciences, Massachusetts Inst. of Technology, 2. Dept. of Geology, Colorado College, 3. Cooperative Inst. for Research in Environmental Sciences, Univ. of Colorado, 4. Dept.of Earth Sciences, Univ. of Minnesota

Symmetric sand ripples formed by shallow water waves are one of the most commonly observed patterns in modern environments and in sedimentary rocks. Because the size and spacing of oscillatory flow sand ripples scale with wave conditions and water depth, ripples preserved in sedimentary rocks are important paleoenvironmental indicators used to infer ancient wave conditions. Previous studies of oscillatory flow bedforms have focused on the development of ripple fields under constant wave forcing or on the transient adjustment of one-dimensional wave ripple profiles to changing flow conditions. However, modern and ancient ripple fields often contain bifurcating ridge crests, short secondary crests formed within major ripple troughs, and other two-dimensional defects -- deviations from straight, evenly spaced ripples. Understanding the formation and evolution of these ripple defects could provide insight to transient wave conditions.

We performed a series of experiments in a field-scale laboratory wave tank to characterize the response of a rippled bed to changes in oscillatory flow. In each experiment, we subjected a level sand bed seeded with small perturbations to constant wave forcing to establish an equilibrium ripple field. We then imposed an abrupt change in wave conditions that would produce a different ripple spacing. Taking shadows in time-lapse images as a proxy for bed elevation, we computed the two-dimensional Fourier power spectrum of the sand bed over the course of each experiment to determine ripple spacing and spectral entropy, a measure of the variability of ripple crest orientation and spacing. We also made qualitative observations of dominant defect types over time. Ripples formed from the initially planar bed were straight crested, evenly spaced, and largely devoid of ripple defects. After wave conditions changed, the ripple bed developed unevenly spaced crests with a variety of defect geometries.

Different types of defects developed to accommodate increases in ripple spacing and decreases in ripple spacing, and some defect types emerged only to accommodate a particular magnitude of change in spacing. In experiments with increases in ripple spacing, cup-like depressions formed on ripple crests and propagated outward to divide existing crests in two and increase ripple spacing. In experiments with minor decreases in ripple spacing, ridge crests became hourglass-shaped, and secondary crests formed within widened trough segments. These secondary crests eventually merged with sinuous or fragmented crests to decrease ripple spacing. In experiments with larger decreases in ripple spacing, secondary crests formed parallel to existing ripple crests then migrated laterally towards the trough to decrease ripple spacing. In some experiments with only small increases or decreases in ripple spacing, defects did not form and the ripple field adjusted by lateral migration of unbroken ripple crests.

As ripple fields reached a new equilibrium spacing, the abundance of defects declined and ripple crests became straighter and more evenly spaced. Yet, some defect types persisted even after the ripple bed attained an average spacing equilibrated to new wave conditions. Crest terminations and tuning fork-shaped bifurcations in ripple crests became the dominant defect type after the main adjustment of ripple fields to either an increase or decrease in spacing. These defects propagated across the bed in the direction of the flow as edge dislocations until the end of our experiments.

Based on these observations, we constructed a regime diagram relating specific ripple defect geometries quantitatively to the sign and magnitude change in ripple spacing and the cumulative sediment transport following the change in wave conditions. These results provide a basis for interpreting different defect types and deciphering the magnitudes and timescales of changing water flow preserved in modern coastal environments and the rock record.

Keywords: Oscillatory flow, Bedforms, Sediment transport

